AIP | Applied Physics Letters

# Molecular beam epitaxy of bilayer Bi(111) films on topological insulator Bi2Te3: A scanning tunneling microscopy study

Mu Chen, Jun-Ping Peng, Hui-Min Zhang, Li-Li Wang, Ke He et al.

Citation: Appl. Phys. Lett. **101**, 081603 (2012); doi: 10.1063/1.4747715
View online: http://dx.doi.org/10.1063/1.4747715
View Table of Contents: http://apl.aip.org/resource/1/APPLAB/v101/i8
Published by the American Institute of Physics.

## Related Articles

Highly ordered self-assembled nanoscale periodic faceting in GaAs(631) homoepitaxial growth
Appl. Phys. Lett. 101, 073112 (2012)

Photoluminescence studies of type-II CdSe/CdTe superlattices
Appl. Phys. Lett. 101, 061915 (2012)

Recrystallization of an amorphized epitaxial phase-change alloy: A phoenix arising from the ashes
Appl. Phys. Lett. 101, 061903 (2012)

Preparation and atomic structure of reconstructed (0001) InGaN surfaces
J. Appl. Phys. 112, 033509 (2012)

Substrate-induced disorder in V2O3 thin films grown on annealed c-plane sapphire substrates
Appl. Phys. Lett. 101, 051606 (2012)

## Additional information on Appl. Phys. Lett.

Journal Homepage: http://apl.aip.org/
Journal Information: http://apl.aip.org/about/about_the_journal
Top downloads: http://apl.aip.org/features/most_downloaded
Information for Authors: http://apl.aip.org/authors

ADVERTISEMENT


Downloaded 21 Aug 2012 to 159.226.35.179. Redistribution subject to AIP license or copyright; see http://apl.aip.org/about/rights_and_permissions

# Molecular beam epitaxy of bilayer Bi(111) films on topological insulator $Bi_2Te_3$: A scanning tunneling microscopy study

Mu Chen,[1,2] Jun-Ping Peng,[1] Hui-Min Zhang,[1] Li-Li Wang,[1] Ke He,[1] Xu-Cun Ma,[1,a)] and Qi-Kun Xue[1,2,a)]
[1]*State Key Laboratory for Surface Physics, Institute of Physics, Chinese Academy of Sciences, Beijing 100190, China*
[2]*State Key Laboratory of Low-Dimensional Quantum Physics, Department of Physics, Tsinghua University, Beijing 100084, China*

(Received 28 May 2012; accepted 7 August 2012; published online 21 August 2012)

We report on molecular beam epitaxy growth of bilayer Bi(111) films on topological insulator $Bi_2Te_3$. *In situ* scanning tunneling microscopy/spectroscopy shows that Bi growth mode changes from quasi bilayer-by-bilayer to step-flow with increasing substrate temperature. Bilayer Bi(111) exhibits an electron donor behavior, causing an 80 meV downshift of the Dirac point of $Bi_2Te_3$. Local work function difference between the bilayer films and $Bi_2Te_3$ films is measured to be 390 meV. Based on the observations, we propose a schematic energy-band diagram which reveals band bending effect at the $Bi/Bi_2Te_3$ interface. Our work paves a way to explore the exotic topological properties of bilayer islands and thin films of Bi. © *2012 American Institute of Physics*. [http://dx.doi.org/10.1063/1.4747715]

Topological insulators[1–3] (TIs) have recently attracted extensive attention due to many exotic properties that come from strong spin-orbital coupling. Topologically protected by time-reversal symmetry, the one-dimensional (1D) edge states in 2D TIs (also called as quantum spin Hall system) and the 2D surface states (SS) in 3D TIs are helical Dirac fermions and immune to backscattering by nonmagnetic impurities and thus promise for future spintronics and quantum computation.[4] Single bilayer (BL) Bi(111) ultrathin film,[5,6] schematically drawn in Fig. 1(a) with a rhombohedral crystal structure, was theoretically predicted to be another category of 2D TIs in addition to the well-known HgTe/CdTe (Ref. 7) and InAs/GaSb (Ref. 8) quantum wells. However, the topological nature has not been proved experimentally. Moreover, it is difficult to achieve epitaxial growth of single BL Bi(111) film on prototype substrates such as Si(001),[9] Si(111),[10] and HOPG.[11] Due to similar layered structure and relatively small in-plane lattice mismatch, $Bi_2Te_3$, $Bi_2Se_3$, and $Sb_2Te_3$ may be good substrates for growing high quality Bi films with sharp interface. By growing Bi on Bi- and Sb-based binary compounds, interface engineering of 2D and 3D TIs may be achieved since these compounds have experimentally been demonstrated to be a nontrivial 3D TI by surface[12–14] and bulk probes.[15–17] Hirahara *et al.*[18] investigated the electronic structure of single BL Bi films grown on $Bi_2Te_3$ by angle-resolved photoemission spectroscopy. However, the growth mechanism and interface structure between Bi and $Bi_2Te_3$ remain unexplored.

In this work, we report on a scanning tunneling microscopy (STM) study of molecular beam epitaxy (MBE) growth of BL Bi(111) islands and thin films on $Bi_2Te_3$(111). We use low temperature (LT) STM to image the real space topography of the Bi islands and thin films. It is found that the growth mode is very sensitive to growth conditions. We carry out scanning tunneling spectroscopy (STS) and local work function (LWF) measurements to characterize the interface band bending effect so that the interface electronic structure can be investigated.

Our experiments are performed with a commercial ultrahigh vacuum (UHV) MBE-STM combined system (Unisoku) with a base pressure better than $1.0 \times 10^{-10}$ Torr. Prior to $Bi/Bi_2Te_3$ deposition, double-layer graphene is prepared on 6 H-SiC(0001)[19] as a smooth and chemically inert substrate by UHV thermal annealing at 1350 °C for 10 min. High-purity Bi (99.999%) and Te (99.9999%) are evaporated from two standard Knudsen diffusion cells (CreaTec), respectively. Following the well-established "van der Waals epitaxy" recipe of $Bi_2Se_3$[13] and $Sb_2Te_3$[14] on graphene, high quality (111)-oriented $Bi_2Te_3$ thin films with a thickness of 15 quintuple layers (QL) can be grown by controlling substrate temperature ($T_{sub}$) and $Te_2/Bi$ flux ratio. The resulted single crystalline films exhibit large terraces of ~100 nm and extremely low point defect density ($\sim 6 \times 10^{10}/cm^2$), on which Bi is deposited under various substrate temperatures. A low deposition rate $J_0 = 0.0937$ BL/min (1 BL = $1.12 \times 10^{15}/cm^2$) of Bi is used. *In situ* STM measurement is conducted at 5.1 K. In order to acquire reliable LWF images and STS spectra by lock-in technique, the STM polycrystalline PtIr tips are calibrated using standard Pb/Si(111) and Ag/Si(111) before and after STM measurement. All STM images are processed by WSxM software.[20]

In order to investigate nucleation and growth of Bi, we first perform room temperature (RT) deposition of Bi on $Bi_2Te_3$(111). A series of STM images ($380 \times 380\ nm^2$) for Bi coverage from 0.2 BL to 1.7 BL are shown in Figs. 1(c)–1(g). At the initial stage of growth (Fig. 1(c)), quasi-equilateral triangular 2D islands with one of the sides parallel to the $Bi_2Te_3$ step edges can be observed. The Bi islands with uniform height of $5.00 \pm 0.10$ Å are almost equally separated. Intuitively, we attribute the three-fold symmetry of islands to

a)Authors to whom correspondence should be addressed. Electronic addresses: xcma@aphy.iphy.ac.cn and qkxue@mail.tsinghua.edu.cn.

 © 2012 American Institute of Physics

Downloaded 21 Aug 2012 to 159.226.35.179. Redistribution subject to AIP license or copyright; see http://apl.aip.org/about/rights_and_permissions

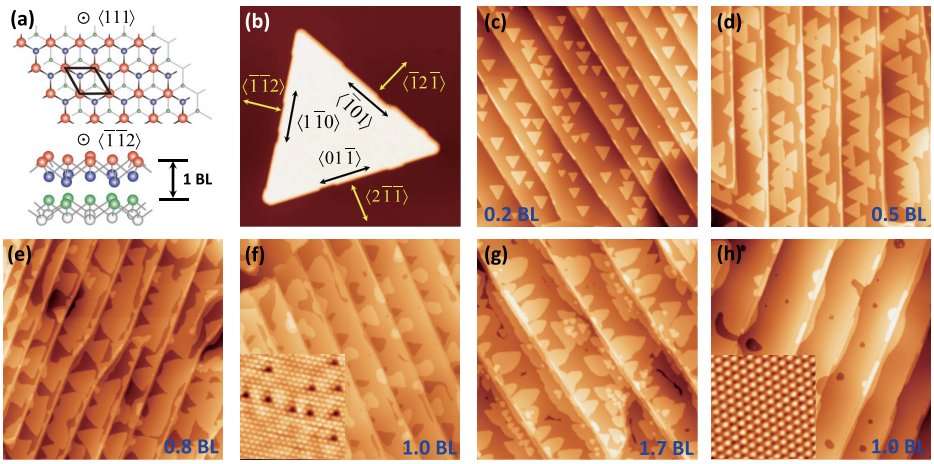


FIG. 1. (a) Crystal structure of single BL Bi(111). Top view and side view are shown. (b) STM image of a quasi-equilateral triangle 1 BL Bi(111) island ($57 \times 57\,nm^2$, setpoint: 1 V, 50 pA). Yellow and black two-way arrows are high symmetry crystal directions. (c)-(g) STM images ($380 \times 380\,nm^2$, setpoint: 4 V, 50 pA) showing gradually increased Bi coverages: 0.2 BL, 0.5 BL, 0.8 BL, 1.0 BL, and 1.7 BL. The inset of (f) shows atomic resolution image of Bi ($8 \times 8\,nm^2$, setpoint: 0.038 V, 200 pA) (h) STM image of 1 BL Bi after annealing at 430 K ($380 \times 380\,nm^2$, setpoint: 4 V, 50 pA). Inset is a high-resolution image of Bi(111) thin film ($5 \times 5\,nm^2$, setpoint: 0.1 V, 100 pA).

hexagonal surface lattice of Bi. Atomically resolved STM image (inset of Fig. 1(f)) indeed reveals the hexagonal structure with an in-plane lattice constant of $4.4 \pm 0.1$ Å. Since the surface unit cell of Bi(110) is rectangular and that of Bi(100) is quasi-hexagonal rhombus,[21] the islands shown in Fig. 1(c) is neither (110)- nor (100)-oriented. The height difference between the first layer and the second layer of Bi is $4.00 \pm 0.10$ Å (Fig. 1(g)) and bias-independent. The value is consistent with the bilayer step height (3.94 Å) of the bulk Bi(111) (a = b = 4.54 Å) along *c* axis.[21] The observation suggests that (111)-oriented Bi films grow on the $Bi_2Te_3$(111) surface.

Interestingly, island edges are preferentially oriented along three directions (⟨1$\bar{1}$0⟩, ⟨$\bar{1}$01⟩, and ⟨01$\bar{1}$⟩) (see black arrows in Fig. 1(b)). The compact quasi-equilateral shape is a result of anisotropic diffusion of Bi adatoms from island corners to the edges, which occurs generally on (111) surface[22,23] under nearly thermodynamic condition. For the coverage of 0.5 BL and above, coalescence of the Bi islands occurs (Fig. 1(d)). Further deposition of Bi leads to growth of the first complete BL films (Figs. 1(e) and 1(f)). We also observe a small amount of the second BL islands, which can be removed by post-growth annealing at ~430 K for hours, as shown in Fig. 1(h). Together with the result for higher coverage such as 1.7 BL in Fig. 1(g), we argue that the RT growth proceeds via a quasi BL-by-BL mode.

On the other hand, growth at elevated temperature ($T_{sub} = 450$ K) proceeds via step-flow mode, leading to an atomically smooth surface of Bi. The situation is shown in a series of STM topographic images for a coverage of 0.3 BL (Fig. 2(a)), 0.5 BL (Fig. 2(c)), 0.9 BL (Fig. 2(d)), and 1.0 BL (Fig. 2(f)), respectively. No clusters or islands can be observed at each step of the growth. The Bi films advance along the direction perpendicular to $Bi_2Te_3$ step, as indicated by white arrows in Fig. 2(a). At 0.9 BL, some part of Bi films reaches upper step edges, eventually a nearly perfect complete bilayer film with very low defect density forms on $Bi_2Te_3$ (Fig. 2(f)). The step-flow growth[24] can be attributed to small Ehrlich-Schwoebel (ES) barrier[25] and thus is thermally activated: at RT, surface mobility of Bi adatoms is limited and the diffusion length is smaller than the terrace width of $Bi_2Te_3$. Thus, they can encounter each other and form a nucleus before arriving at step edges. At 450 K, the diffusion of Bi adatoms is promoted and most of them can reach the step edge given the same small ES barrier. In this case, the growth proceeds via adatom incorporation at the

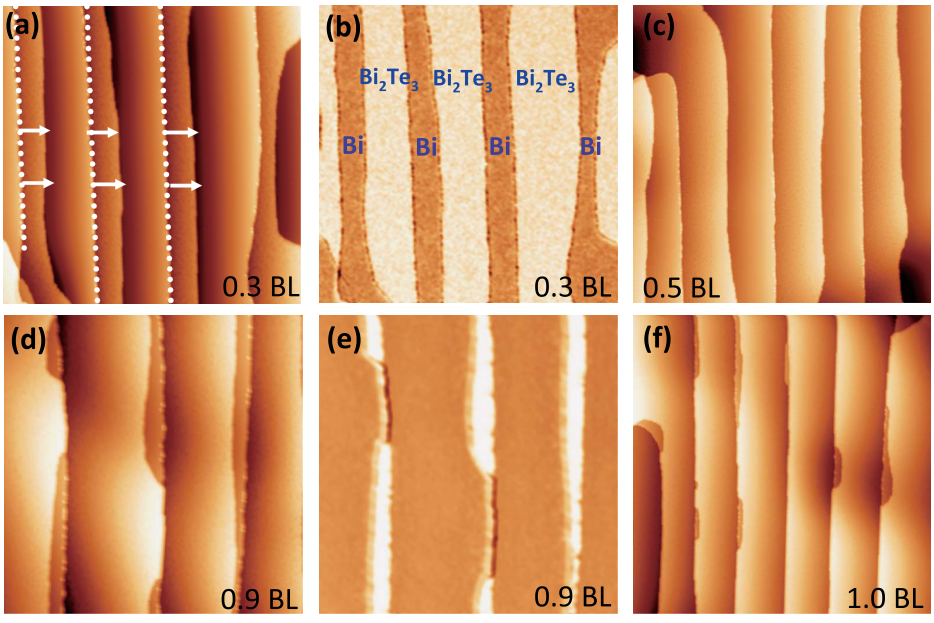


FIG. 2. STM and LWF images showing different coverages of Bi(111) thin films on $Bi_2Te_3$ as $T_{sub} = 450$ K: (a) 0.3 BL, (c) 0.5 BL, (d) 0.9 BL, and (f) 1.0 BL. ($220 \times 220\,nm^2$, setpoint: 0.3 V, 100 pA). (b) and (e) are LWF images simultaneously acquired with (a) and (d), respectively. AC voltage modulation of z-scan piezo: $V_{rms} = 10$ mV, frequency = 2997 Hz. Dashed lines in (a) are guide to the eyes to mark the boundaries between Bi and $Bi_2Te_3$.

Downloaded 21 Aug 2012 to 159.226.35.179. Redistribution subject to AIP license or copyright; see http://apl.aip.org/about/rights_and_permissions

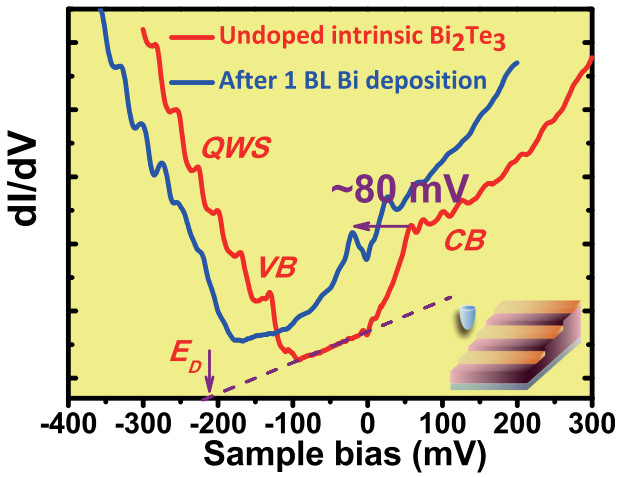


FIG. 3. *dI*/*dV* spectra taken on as-grown $Bi_2Te_3$ with a thickness of 15 quintuple layers (red), and bare places of $Bi_2Te_3$ after 1 BL Bi film deposition in Fig. 2(f) (blue). The purple arrows are indications of rigid LDOS shift with respect to energy ~80 meV. (setpoint: 200 mV, 200 pA). The bias modulation is 3 $mV_{rms}$ at 987.5 Hz.

step edge. We also find that there is no chemical reaction between Bi and Te-terminated $Bi_2Te_3$ in the temperature range from 300 K to ~450 K. If $T_{sub}$ is greater than 450 K, evaporation of Bi from the surface occurs, while at LT (for example $T_{sub} \leq 150$ K) Bi clusters with a typical size of ~3 nm form (not shown). Therefore, the step-flow growth of Bi films occurs in a temperature range of 300 K–450 K.

Next, we discuss the electronic structure of $Bi/Bi_2Te_3$ interface. For the step-flow mode, it is difficult to identify which part is the growing Bi films from the topographic images alone. We then carry out LWF measurement.[26] According to quantum tunneling theory, the tunneling current $I$ decays exponentially with tip-sample separation z as $I \propto \exp\left(-\frac{\sqrt{8m\Phi_{eff}}}{\hbar} z\right)$. Then

$$\Phi_{eff} = \frac{\hbar^2}{8m}\left(\frac{d\ln I}{dz}\right)^2. \quad (1)$$

$\Phi_{eff}$ is an effective barrier height and can be approximately expressed as[27]

$$\Phi_{eff} = (\Phi_{sample} + \Phi_{tip} - e|V_{bias}|)/2, \quad (2)$$

where $\Phi_{sample}$ and $\Phi_{tip}$ are the WF of the sample and tip, respectively, and $V_{bias}$ is the tunneling bias voltage. If an *ac* voltage is superimposed on the z-scan piezo, response tunneling current is collected and $\frac{d\ln I}{dz}$ signal can be acquired via lock-in technique. This way $\Phi_{sample}$ is deduced by Eq. (2). Figs. 2(b) and 2(e) are the corresponding LWF images of Figs. 2(a) and 2(d), respectively, from which one can immediately tell that the dark contrast part is Bi. The alternative bright and dark regions correspond to the WF contrast of $\Phi_{Bi_2Te_3}$ and $\Phi_{Bi}$, respectively. Since the work function of the 15 QL thin films is very close to the bulk value due to the layered structure and unreconstructed film surface of $Bi_2Te_3$, we use the bulk value of $\Phi_{Bi_2Te_3} = 5.3$ eV (Refs. 28 and 29) for the thin films and obtain $\Phi_{Bi} = 4.91$ eV for the first BL Bi. The results are confirmed with different tunneling setpoints and voltage modulation parameters and on 1 BL Bi islands.[30]

Local density of states (LDOS) of the $Bi_2Te_3$ sample is shown in Fig. 3 (red curve). The onsets of bulk conduction band (BCB) and bulk valence band (BVB) are around 58 meV and −130 meV relative to Fermi level ($E_F$), respectively. Quantum well states of BVB, similar to $Sb_2Te_3$,[14] are clearly identified. Pure SS exist in the bulk energy gap ($E_g$) between BCB and BVB. Since it is energetically buried in BVB, the Dirac point ($E_D$) of $Bi_2Te_3$ can only be obtained indirectly by extending the pure SS to bias axis (the intercept). After Bi deposition (Fig. 2(f)), spatially averaged *dI*/*dV* spectra (blue line in Fig. 3) are taken locally on the exposed $Bi_2Te_3$ region (not covered by Bi). LDOS curve shifts rigidly to lower energy and $E_D$ is moved from −210 meV to −290 meV. Surface charge density contributed by SS scales as $n = \frac{1}{4}E_D^2/[\pi(\hbar v_F)^2]$. After 1 BL Bi deposition, the charge density changes to $6.58 \times 10^{12}/cm^2$, which is nearly twice the value of bare $Bi_2Te_3$ ($3.45 \times 10^{12}/cm^2$). Note that $E_F$ is now located in BCB so that a large amount of bulk carriers are induced by Bi. The result indicates an n-type doping and charge transfer from Bi to $Bi_2Te_3$.

Based on the above observations, we propose a schematic energy-band diagram at the interface. Noncontact condition

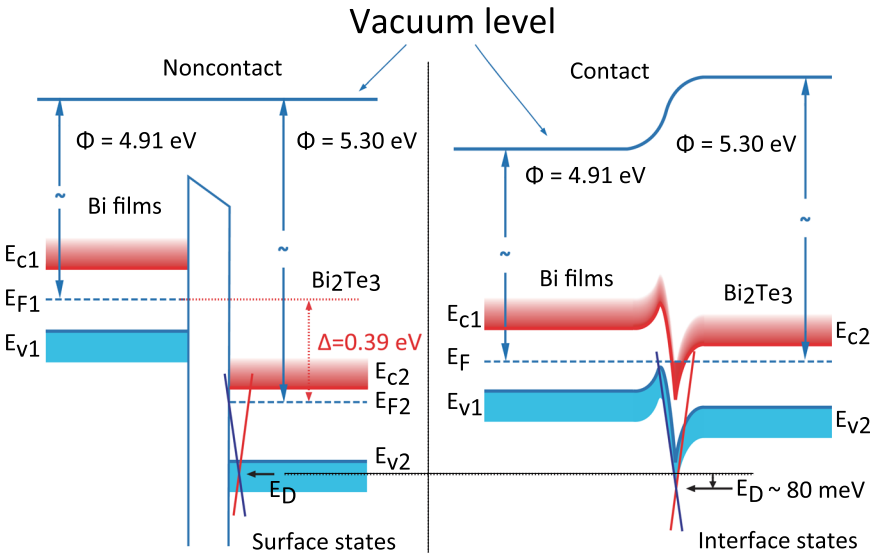


FIG. 4. A semi-quantitative energy-band diagram of the interface between Bi films and $Bi_2Te_3$ films: noncontact (left panel) and contact (right panel) conditions.

Downloaded 21 Aug 2012 to 159.226.35.179. Redistribution subject to AIP license or copyright; see http://apl.aip.org/about/rights_and_permissions

between two films is shown in the left part of Fig. 4. Single BL Bi thin film is considered to be a semiconductor (except the edges) with $E_g \sim 160$ meV (Ref. 6) and its $E_F$ lies in the middle of $E_g$. The WF of 1 BL Bi is 4.91 eV, which is defined as the energy difference between $E_F$ and the vacuum level. Meanwhile, $Bi_2Te_3$ is n-type TI with a direct bulk $E_g \sim 188$ meV as revealed by STS, its $E_F$ is near the bottom of BCB. The WF difference (the $E_F$ difference) between Bi and $Bi_2Te_3$ is 390 meV. Under contact condition (see the right part of Fig. 4), $E_F$ of Bi and $Bi_2Te_3$ are aligned to the same level. To respond to the band shift ~80 meV in STS measurement, BCB, interface states (in contrast to SS in noncontact condition) and BVB of $Bi_2Te_3$ have to shift downward in real space. The strong band bending trend is consistent with large WF difference of 390 meV between $Bi_2Te_3$ and Bi. It also causes the bottom of BCB moving below $E_F$ so that bulk electrons flow from Bi into $Bi_2Te_3$. We speculate that the electrons may be confined in the triangular potential well but can move freely parallel at the interface so that a built-in electric field vertical to the interface may occur. Moreover, Dirac electron density contributing to interface states is doubled. This abrupt Bi-$Bi_2Te_3$ interface may serve as an electronic band engineering device, which can be applied to both bulk and SS electrons.

In summary, atomically flat single bilayer Bi(111) films are heteroepitaxially grown on $Bi_2Te_3$. Combined with real space LWF imaging and STS measurement, band bending effect between the interface is revealed. The work paves a material foundation for further study of the topological edge/surface states of Bi and Bi/$Bi_2Te_3$ heterostructure. Extension to other systems such as $Bi_2Se_3$ and $Sb_2Te_3$ is envisioned.

This work was supported by China's National Science Foundation, the Ministry of Science and Technology of China, and the Chinese Academy of Sciences.

[1]X.-L. Qi and S.-C. Zhang, Phys. Today **63**(1), 33 (2010).
[2]X.-L. Qi and S.-C. Zhang, Rev. Mod. Phys. **83**, 1057 (2011).
[3]M. Z. Hasan and C. L. Kane, Rev. Mod. Phys. **82**, 3045 (2010).
[4]J. E. Moore, Nature **464**, 194 (2010).
[5]S. Murakami, Phys. Rev. Lett. **97**, 236805 (2006).
[6]M. Wada, S. Murakami, F. Freimuth, and G. Bihlmayer, Phys. Rev. B **83**, 121310 (2011).
[7]M. Konig, S. Wiedmann, C. Brune, A. Roth, H. Buhmann, L. W. Molenkamp, X.-L. Qi, and S.-C. Zhang, Science **318**, 766 (2007).
[8]I. Knez, R.-R. Du, and G. Sullivan, Phys. Rev. Lett. **107**, 136603 (2011).
[9]G. Jnawali, H. Hattab, C. A. Bobisch, A. Bernhart, E. Zubkov, R. Moller, and M. Horn-von Hoegen, Surf. Sci. **603**, 2057 (2009).
[10]T. Nagao, J. T. Sadowski, M. Saito, S. Yaginuma, Y. Fujikawa, T. Kogure, T. Ohno, Y. Hasegawa, S. Hasegawa, and T. Sakurai, Phys. Rev. Lett. **93**, 105501 (2004).
[11]P. J. Kowalczyk, O. Mahapatra, D. N. McCarthy, W. Kozlowski, Z. Klusek, and S. A. Brown, Surf. Sci. **605**, 659 (2011).
[12]T. Zhang, P. Cheng, X. Chen, J.-F. Jia, X.-C. Ma, K. He, L. L. Wang, H.-J. Zhang, X. Dai, Z. Fang, X.-C. Xie, and Q.-K. Xue, Phys. Rev. Lett. **103**, 266803 (2009).
[13]P. Cheng, C. L. Song, T. Zhang, Y. Y. Zhang, Y. L. Wang, J.-F. Jia, J. Wang, Y.-Y. Wang, B.-F. Zhu, X. Chen, X.-C. Ma, K. He, L. L. Wang, X. Dai, Z. Fang, X.-C. Xie, X.-L. Qi, C.-X. Liu, S.-C. Zhang, and Q.-K. Xue, Phys. Rev. Lett. **105**, 076801 (2010).
[14]Y. P. Jiang, Y. Y. Sun, M. Chen, Y. L. Wang, Z. Li, C. L. Song, K. He, L. L. Wang, X. Chen, Q.-K. Xue, X.-C. Ma, and S. B. Zhang, Phys. Rev. Lett. **108**, 066809 (2012).
[15]D.-X. Qu, Y. S. Hor, J. Xiong, R. J. Cava, and N. P. Ong, Science **329**, 821 (2010).
[16]J. G. Analytis, R. D. McDonald, S. C. Riggs, J.-H. Chu, G. S. Boebinger, and I. R. Fisher, Nat. Phys. **6**, 960 (2010).
[17]D. S. Kong, Y. L. Chen, J. J. Cha, Q. F. Zhang, J. G. Analytis, K. J. Lai, Z. K. Liu, S. S. Hong, K. J. Koski, S.-K. Mo, Z. Hussain, I. R. Fisher, Z.-X. Shen, and Y. Cui, Nat. Nanotechnol. **6**, 705 (2011).
[18]T. Hirahara, G. Bihlmayer, Y. Sakamoto, M. Yamada, H. Miyazaki, S. Kimura, S. Blugel, and S. Hasegawa, Phys. Rev. Lett. **107**, 166801 (2011).
[19]J. Hass, W. A. de Heer, and E. H. Conrad, J. Phys.: Condens. Matter **20**, 323202 (2008).
[20]I. Horcas, R. Fernandez, J. M. Gomez-Rodriguez, J. Colchero, J. Gomez-Herrero, and A. M. Baro, Rev. Sci. Instrum. **78**, 013705 (2007).
[21]Ph. Hofmann, Prog. Surf. Sci. **81**, 191 (2006).
[22]T. Michely, M. Hohage, M. Bott, and G. Comsa, Phys. Rev. Lett. **70**, 3943 (1993).
[23]M. Hohage, M. Bott, M. Morgenstern, Z.-Y. Zhang, T. Michely, and G. Comsa, Phys. Rev. Lett. **76**, 2366 (1996).
[24]J. R. Arthur, Surf. Sci. **500**, 189 (2002).
[25]M. G. Lagally and Z. Y. Zhang, Nature **417**, 907 (2002).
[26]Y. Qi, X. Ma, P. Jiang, S. H. Ji, Y. S. Fu, J.-F. Jia, Q.-K. Xue, and S. B. Zhang, Appl. Phys. Lett. **90**, 013109 (2007).
[27]J. Kim, S. Y. Qin, W. Yao, Q. Niu, M. Y. Chou, and C. K. Shih, Proc. Natl. Acad. Sci. U.S.A. **107**, 12761 (2010).
[28]D. Haneman, J. Phys. Chem. Solids **11**, 205 (1959).
[29]In LWF images, $\frac{d\ln I}{dz}$ values of single BL Bi films and $Bi_2Te_3$ are given. Since $\Phi_{eff} = \frac{\hbar^2}{8m}\left(\frac{d\ln I}{dz}\right)^2 = (\Phi_{sample} + \Phi_{tip} - e|V_{bias}|)/2$, then $\frac{\Phi_{Bi_2Te_3}+\Phi_{tip}-e|V_{bias}|}{\Phi_{Bi}+\Phi_{tip}-e|V_{bias}|}$ equals to $\left[\frac{d(\ln I)/dz(Bi_2Te_3)}{d(\ln I)/dz(Bi)}\right]^2$. Finally $\Phi_{Bi}$ is precisely extracted.
[30]In order to rule out tip induced uncertainty in obtaining $\Phi_{Bi}$, we shift bias from +0.3 V to −0.3 V, tunneling current from 50 pA to 200 pA, frequency of *ac* voltage from 2997 Hz to 1997 Hz. LWF imaging are also carried out on 1 BL equilateral triangular Bi islands. All the results generate $\Phi_{Bi} = 4.91 \pm 0.01$ eV.

Downloaded 21 Aug 2012 to 159.226.35.179. Redistribution subject to AIP license or copyright; see http://apl.aip.org/about/rights_and_permissions